Effects of cation field strength on the structure of aluminoborosilicate glasses: High-resolution ^{11}B, ^{27}Al and ^{23}Na MAS NMR

Jingshi Wu*, Jonathan F. Stebbins

Dept. of Geological and Environmental Sciences, Stanford University, 450 Serra Mall, Building 320, Stanford, CA 94305, United States

ABSTRACT

Among the most important adjustable compositional variables in controlling glass and glass-melt properties are the relative proportions of network modifiers with varying cation field strength (ratio of charge to radius). Here we determine the details of structural changes caused by variations in the ratio CaO/Na_2O in two series of aluminoborosilicate glasses with different contents of boron oxide. Using high-resolution, high field ^{11}B and ^{27}Al MAS NMR, we report precise values of contents of three- and four-coordinated boron (N_4) and of four- and five-coordinated aluminum ([5]Al), and calculate fractions of non-bridging oxygens (NBOs). Increasing CaO/Na_2O dramatically lowers N_4 and increases NBO and [5]Al, but effects are non-linear with composition. Boron content affects these trends because of energetic constraints of mixing of various network cations. [23]Na spectra reveal slight but systematic increases in the mean Na–O distance with increasing CaO/Na_2O, suggesting that in Ca-rich glasses, Na^+ has a higher ratio of bridging to non-bridging oxygens in its coordination shell. All of these changes can be understood by the tendency of higher field strength modifier cations to promote the concentration of negative charges on non-bridging oxygens in their local coordination environment, systematically converting four- to three-coordinated boron.

© 2009 Elsevier B.V. All rights reserved.

1. Introduction

Multicomponent aluminoborosilicate glasses are widely used in technologies such as flat panel display substrates, fiber glass, photochromic glass, and the sequestration of radioactive waste [1–10]. Many studies have documented the close relationships between physical properties and structure of boron-containing glasses [11–18]. Extensive efforts have also been made to model the effects of composition on properties [19–21], many of which are based on structural speciation reactions [22–27].

When network modifier oxides are added to pure silica, the silicate framework 'depolymerizes' through the formation of non-bridging oxygen (NBO), while most or all Si remains four-coordinated. In contrast, when modifiers are initially added to boric-oxide glass, the added oxide ion is accommodated by the conversion of trigonal boron ([3]B) to tetrahedral boron ([4]B) with little or no formation of NBO. If enough alkali oxide is added, tetrahedral boron begins to convert to asymmetric trigonal boron groups, which contain one NBO and two bridging oxygens (BO) [28]. An early statistical thermodynamic model of this process

[24] allowed the calculation of the fraction of four-coordinated boron among total boron species (N_4) as a function of composition and temperature in alkali borate glasses and glass-forming liquids. In sodium borosilicates, the maximum value of N_4 increases with silica content, as described by the frequently-used empirical model of Dell et al. [28], and most NBO are bonded to Si instead of to B. The ease with which boron can change between three and four coordination as composition and temperature are changed, thus has a major influence on properties such as viscosity, melting points, and glass transition temperatures.

Constraints on boron coordination in glasses come mostly from NMR, beginning with many early 'wideline' NMR studies [27–31], then more recently with high field and high-resolution ^{11}B MAS NMR [32–36]. Compositional effects on N_4 are now especially well-known for alkali borosilicates, but more complex systems are less well-understood. Some studies [2,3,37–41] have begun to systematize the structural changes caused by adding Al_2O_3 to borosilicates. Aluminum in these compositions generally is predominantly [4]Al, but high field ^{27}Al NMR spectra have revealed the added complication of significant [5]Al, especially in glasses with divalent modifier cations [39,42]. Despite these efforts, the systematic effects of one of the most commonly used compositional variations, the field strength of the modifier cation, have only been

* Corresponding author.
E-mail address: jswu@stanford.edu (J. Wu).

explored in a few aluminoborosilicate systems. For example, Yamashita et al. [3], in comparing K, Na, Ba, Sr, Ca, and Mg aluminoborosilicates, noted that the smaller, higher charged cations systematically increased the NBO content and decreased N_4 for a given Al/B ratio [3].

As discussed in recent studies that included ^{17}O NMR, oxygen speciation is closely linked to the network structure [41,43,44]. In a simple silicate melt, NBOs are formed stoichiometrically on addition of modifier oxide to silica (assuming negligible 'free' O^{2-} ions), as expressed by the structure 'reaction':

$$SiO_{4/2} + 1/2O^{2-} = [SiO_{3/2}O]^{-}, \tag{1}$$

$[SiO_{3/2}O]^{-}$ indicates a four-coordinated silicon with three bridging oxygens and one NBO, where $O_{x/y}$ denotes x oxygen anions, each coordinated with y network cations, e.g., a bridging oxygen when $y = 2$. In an aluminosilicate, some modifier oxide instead contributes oxygen to form $^{[4]}$Al and cations to charge balance the underbonded bridging oxygens such as Al–O–Si. Again, if the contents of $^{[5]}$Al, $^{[6]}$Al and oxygen triclusters are negligible, NBO content can be deduced directly from stoichiometry. In boron-containing systems, there is an interplay between oxygen and boron speciation that can be expressed by schematic reactions such as:

$$BO_{3/2} + NBO^{-} = [BO_{4/2}]^{-}, \tag{2}$$

or, more precisely for borosilicates:

$$BO_{3/2} + SiO_{3/2}O^{-} = [BO_{4/2}]^{-} + SiO_{4/2}, \tag{3}$$
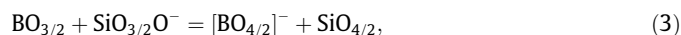
In the types of compositions studied here, most of the NBO are associated with Si instead of with B as shown directly by ^{17}O NMR [42,50], but a complete thermodynamic formulation would of course include both types of species. At low contents of modifier oxides in boron-rich glasses, these reactions are nearly complete [24,28,29]. At high modifier contents the equilibrium tends to shift back, in part because of the relative energetic unfavorability of $^{[4]}$B–O–$^{[4]}$B linkages [14,45], which in turn can be mitigated by dilution with silica [25,28,46,47]. Higher temperature or higher modifier cation field strength, which favor the formation of NBO, pushes the reaction to the left [42,48–50].

In this paper we isolate a key compositional variable, one that is commonly exploited in the tailoring of glass and glass-forming melt properties to particular applications, by selecting two aluminoborosilicate compositional joins in which Na_2O is substituted for CaO. Thus, total oxygen ion content remains identical, and only the charge and number of modifier cations changes. We use ^{11}B, ^{27}Al and ^{23}Na MAS NMR to determine changes in both network speciation and modifier cation environment as a function of the Na_2O/CaO ratio at two different ratios of B_2O_3 to SiO_2. We deduce the corresponding changes in oxygen speciation, and show that it is likely that the effect of modifier cation charge on the oxygen speciation is the most important drive in controlling the boron speciation, which in turn has important effects on melt viscosity, glass transition behavior, and corrosion resistance.

2. Experimental

2.1. Sample preparation

Ten glass samples were synthesized with composition $20M^{n+}_{2/n}O \cdot 8Al_2O_3 \cdot 7B_2O_3 \cdot 65SiO_2$ and $20M^{n+}_{2/n}O \cdot 8Al_2O_3 \cdot 21B_2O_3 \cdot 51SiO_2$ (M = Na and Ca), where Na_2O/(Na_2O + CaO) = 0, 0.25, 0.5, 0.75 and 1 (Table 1). The Na and Ca end members were made using appropriate amounts of dried $CaCO_3$, Na_2CO_3, Al_2O_3, B_2O_3 and SiO_2. Approximately 0.1 wt% of Co_3O_4 was added to each 2 g sample to speed spin-lattice relaxation, permitting more rapid data collection during NMR experiments. To make the Na-containing glasses (denoted as B7N20 and B21N20), the starting materials were mixed thoroughly and heated at 600 °C for 10 h to allow decarbonation. Each mixture was then packed into a Pt tube with both ends welded to prevent alkali loss during melting. The samples were melted at 1300 °C for 30 min, and then quenched by dipping the Pt capsule into water. For the Ca-containing glasses (denoted as B7N00 and B21N00), the mixtures were heated at 700 °C for 10 h for decarbonation, followed by melting in sealed Pt tubes at 1400 °C for 30 min and water quenching. The samples with intermediate compositions were synthesized by mixing the appropriate amounts of the two end members and remelting at 1400 °C for 30 min.
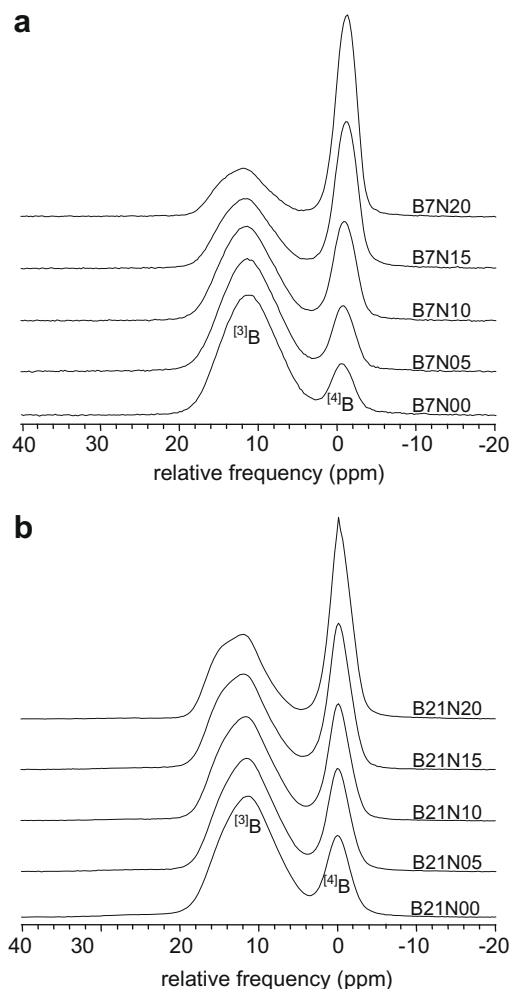
2.2. NMR data collection and analysis

^{11}B MAS NMR spectra were collected on a Varian 14.1 T spectrometer at 192.4 MHz using a Varian/Chemagnetics T3 probe with 3.2 mm zirconia rotors spinning at 20 kHz with a recycle delay of 1 s and a radio frequency pulse length of 0.3 μs, which corresponds to a radiofrequency (rf) tip angle for solids of 20°. ^{11}B chemical shifts are reported in parts per million (ppm) relative to 1.0 M boric acid at 19.6 ppm. ^{27}Al MAS NMR spectra were collected on a Varian 18.8 T spectrometer at 208.4 MHz with 0.2 s delay and 0.2 μs pulse length (solid 30° rf tip angle), also using a T3 probe with similar rotors spinning at 20 kHz, with chemical shift relative to 0.1 M aqueous $Al(NO_3)_3$ at 0 ppm. ^{23}Na MAS NMR spectra were collected at both 14.1 and 18.8 T with 30° (solid) rf tip angles, spinning speeds of 20 kHz, and were referenced to a 1.0 M NaCl solution at 0 ppm. ^{29}Si spectra are not reported, as for these types of multicomponent glasses they are completely unresolved [50], making analysis in terms of silicate species highly model-dependent [3].

3. Results

3.1. ^{11}B MAS NMR

^{11}B MAS NMR peaks corresponding to $^{[3]}$B and $^{[4]}$B groups (centered around 12 and 0 ppm, respectively, Fig. 1) are well-resolved in spectra of the glasses at 14.1 T. The peaks were each fit with two

Table 1
Nominal compositions of samples, in mol%.

Series	Sample	Na$_2$O	CaO	B$_2$O$_3$	Al$_2$O$_3$	SiO$_2$
B7	B7N20	20	0	7	8	65
	B7N15	15	5	7	8	65
	B7N10	10	10	7	8	65
	B7N05	5	15	7	8	65
	B7N00	0	20	7	8	65
B21	B21N20	20	0	21	8	51
	B21N15	15	5	21	8	51
	B21N10	10	10	21	8	51
	B21N05	5	15	21	8	51
	B21N00	0	20	21	8	51

a

b

Fig. 1. [11]B MAS spectra for the low boron series (a) and high boron series (b) glasses collected at 14.1 T. The intensity of each spectrum is normalized to the same total peak area.

Gaussians because of their non-symmetric lineshapes. These pairs were summed for each boron coordination number with no attribution of structural significance. The relative populations of the two sites (Table 2) can be easily determined from these peak areas after correction for the intensity of the satellite transition spinning sidebands that are hidden under the central peaks. Peaks corresponding to [4]B increase in intensity with increasing $Na_2O/(Na_2O + CaO)$, but the fraction of the tetrahedral boron species (N_4) is not an exact linear function of composition and cation field

strength (Fig. 4). When both Na and Ca cations are present, N_4 is somewhat lower than would be expected from linear combinations of the appropriate end members. A similar 'mixed cation effect' also has been observed in alkali borate glasses [51] and, for Al species, in high-pressure aluminosilicate glasses [52]. Boron coordination changes from predominantly trigonal to mostly tetrahedral as $Na_2O/(Na_2O + CaO)$ increases, and the effect of this compositional variable in the B7 series is larger than in the B21 series. With higher boron content, there is more [4]B at the Ca-rich end of the join but less at the Na-rich end.

3.2. ^{27}Al MAS NMR

The ^{27}Al MAS NMR spectra of low boron and high boron glasses collected at 18.8 T are shown in Fig. 2. This very high field provides better resolution and quantification of peaks for [4]Al and [5]Al (and [6]Al, if present), because second-order quadrupolar broadening is reduced. The spectra consist of signals from two aluminum environments: the peak maximum for the predominant [4]Al is at about 60 ppm and that of the minor [5]Al is at about 30 ppm. (The small peaks at about 0 ppm are due to a background signal from the rotors.) The [4]Al and [5]Al peaks both have typical asymmetric forms with tails extending towards lower frequency resulting from distributions in quadrupolar coupling constants. These were each fit with two Gaussians to approximate this line shape and the relative intensities determined by integration.

a

b
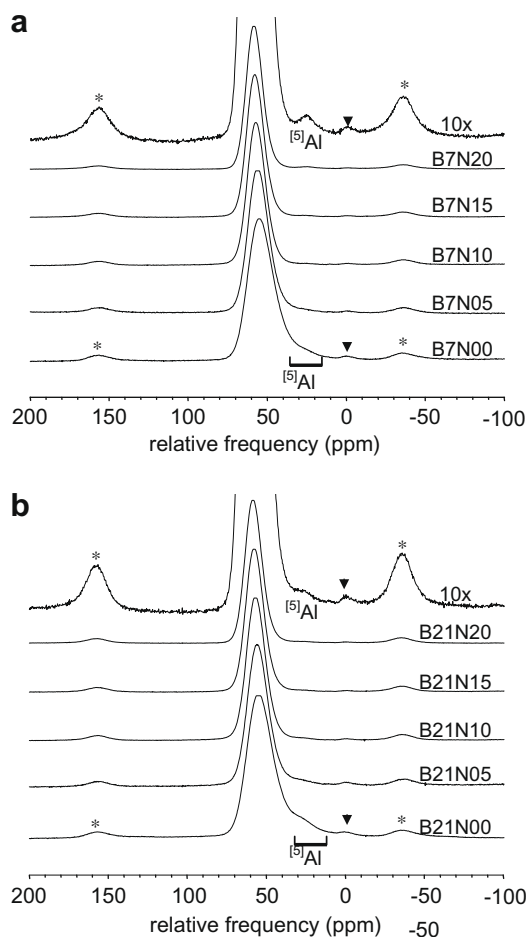
Fig. 2. [27]Al MAS spectra for the low boron series (a) and high boron series (b) glasses collected at 18.8 T. The intensity of each spectrum is normalized to that of its highest peak. The top spectra for (a) and (b) are B7N20 and B21N20 with a vertical scale ×10, respectively. Asterisks denote spinning sidebands. Triangle marks rotor background.

Table 2
NMR results for fractions of [4]B and [5]Al, and calculated NBO fractions among total oxygens.

Sample	N_4[a]	[5]Al[b]	NBO[c]	Sample	N_4[a]	[5]Al[b]	NBO[c]
B7N00	0.15	0.06	0.117(1)	B21N00	0.21	0.14	0.084(3)
B7N05	0.19	0.02	0.111(1)	B21N05	0.27	0.06	0.064(3)
B7N10	0.28	0.01	0.103(1)	B21N10	0.32	0.03	0.053(3)
B7N15	0.44	0.01	0.092(1)	B21N15	0.36	0.01	0.044(3)
B7N20	0.62	0.01	0.080(2)	B21N20	0.51	0.01	0.014(4)

[a] Uncertainties are about ±5% of reported values, based on reproducibility of fitting and integration.
[b] [5]Al is fraction of [5]Al in aluminum species. Uncertainties are about ±30% of reported values.
[c] Uncertainties (in last decimal place as shown) for the fractions of NBO are based on uncertainties for N_4 and [5]Al.

[5]Al is a minor, but measurable, component for all compositions, but becomes more significant in the glasses with the highest Ca/Na ratios (Table 2). In the Ca-rich samples, [5]Al increases with increasing cation field strength, and the change appears to be non-linear with composition (Table 2). The amount of [5]Al in the Ca-rich glasses is higher in the higher boron series. Higher field strength cations are also known to promote the formation of [5]Al in aluminoborate glasses [53,54].

3.3. ^{23}Na MAS NMR

Fig. 3 shows the ^{23}Na MAS spectra of the Na-containing glasses collected at 18.8 T; data were also obtained at 14.1 T. Each spectrum contains a single, broad, asymmetrical peak, whose maximum shifts to lower frequency as the Ca/Na ratio increases. Especially at the high field of 18.8 T, distributions of chemical shifts due to variations in Na environments (for example varying fractions of BO and NBO neighbors) significantly affect the peak shapes, although analyzing this structural information is complicated by the relatively high coordination number of Na$^+$ [55]. In contrast, ^{23}Na spectra collected at lower fields generally have 'tails' to low frequency that are controlled primarily by distributions in quadrupolar coupling constants and are thus less informative about structure. Data obtained at different magnetic fields can, however, readily be used to estimate the mean isotropic chemical shift (δ_{iso}) and the mean quadrupolar coupling constant (C_q) because the center of gravity (δ_{cg}, in ppm) of the resonance is related to the true isotropic chemical shift by the equation [56,57]:

$$\delta_{cg} = \delta_{iso} - \left(C_q^2/40\nu_0^2 \right)\left(1 + \eta^2/3\right)10^6.$$

Here, ν_0 is the Larmor frequency and η is the quadrupolar asymmetry parameter. The latter was chosen rather arbitrarily as 0.7 in all calculations, but variation of η over its full range (0–1) would result in only ~15% variations in the derived C_q values. Data for δ_{cg} at 18.8

Table 3
Peak positions and mean values of chemical shifts and quadrupolar parameters derived from ^{23}Na NMR.

Sample	$\delta_{cg} \pm 0.5$ ppm 14.1 T	$\delta_{cg} \pm 0.3$ ppm 18.8 T	$\delta_{iso} \pm 0.5$ ppm	$C_q \pm 0.2$ MHz
B7N20	−13.9	−9.5	−3.8	3.0
B7N15	−15.3	−11.1	−5.7	2.9
B7N10	−16.6	−12.7	−7.7	2.8
B7N05	−17.6	−14.2	−9.8	2.6
B21N20	−14.5	−10.4	−5.1	2.9
B21N15	−16.0	−11.6	−5.9	3.0
B21N10	−17.0	−13.0	−7.9	2.8
B21N05	−17.9	−14.0	−9.0	2.8

δ_{cg} is the center of gravity in ppm. C_q was calculated using $\eta = 0.7$; the uncertainty is estimated allowing for the fact that η can vary between 0 and 1.

and 14.1 T, and calculated values for means of δ_{iso} and C_q are given in Table 3. The chemical shifts become significantly higher (less negative) with increasing Na/Ca. Because there is a negative correlation between δ_{iso} and mean Na–O bond distance [58], this result indicates that such distances on average are longer in high Ca vs. high Na glasses. From published correlations for silicates, a decrease in chemical shift of about 5 ppm suggests an increase of about 0.01 nm [58–60]. Similar correlations were found for sodium borates and for sodium germanates [61]. The overall change in mean chemical shift is slightly larger in the B7 series (−3.8 to −9.8 ppm) than in the B21 series (−5.1 to −9.0 ppm), perhaps because of the relatively low NBO content in the Na-rich glasses of the latter series (see next section). The estimated mean C_q values tend to decrease with increasing Ca/Na, especially in the B7 series (Table 3), suggesting less distortion from local spherical symmetry, and contributing to the observed slight decreases in peak widths.

3.4. Oxygen speciation

The conversion of [3]B to [4]B consumes NBO to form bridging oxygens. If all Al is [4]Al, and oxygen triclusters are negligible, the NBO fraction can thus be calculated directly from concentrations of [4]B and [4]Al measured by NMR and oxygen mass balance, regardless of whether NBO are on Si, B, or Al [42]. The number of
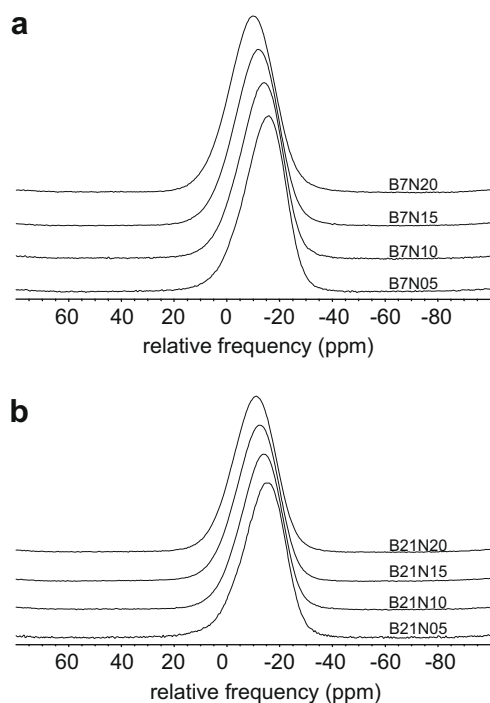
Fig. 3. ^{23}Na MAS spectra for the low boron series (a) and high boron series (b) glasses collected at 18.8 T. The intensity of each spectrum is normalized to that of its highest peak.
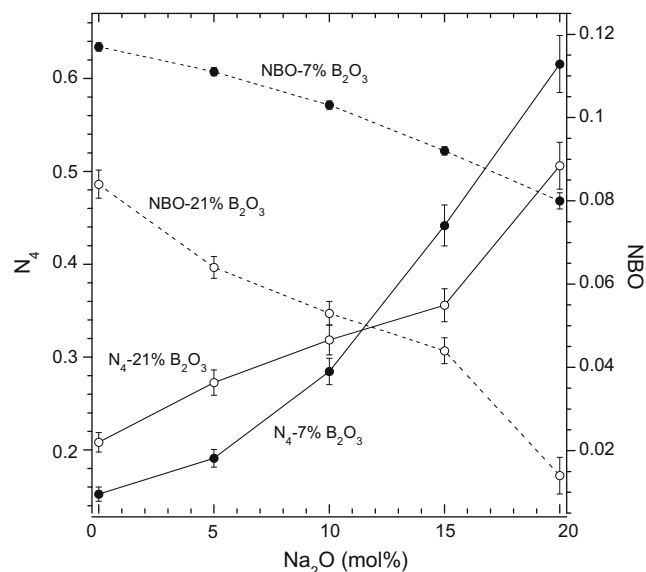
Fig. 4. NMR results for two series of aluminoborosilicate glass. N_4 is fraction of [4]B, NBO is non-bridging oxygen content. Solid lines connect N_4 data, and dashed lines connect fraction of NBOs. Solid circle is B7 series, and open circle is B21 series.

NBO per formula unit is simply $2 \times$ (mol% of $M_{2/n}^{n+}$O – mol% of [4]B – mol% of [4]Al), which, when divided by the total number of oxygens per formula unit (195 for the B7 series, 209 for the B21 series), gives the fraction of NBO among all oxygens. If [5]Al is present, the oxygen speciation will be more complex [62,63]. However, if [5]Al is low, as here, we can simply use measured [4]Al in this equation. The proportions of [4]B and NBO are listed in Table 2 and plotted in Fig. 4. The figure clearly shows the dramatic effects of Ca vs. Na on the oxygen speciation. Also, because N_4 is non-linear with composition, NBO is non-linear, with contents slightly higher in mixed glasses than expected from interpolation between end members.

4. Discussion

4.1. Effect of modifier cation on network cation coordination

Fig. 4 summarizes the major effects of increasing CaO/Na$_2$O ratio on decreasing N_4 and increasing NBO contents for our samples with two different ratios of SiO$_2$/B$_2$O$_3$. Such effects are known in general from previous studies, where Ca^{2+} has been described as having a greater effect on 'depolymerizing' the borosilicate network [3,42,64]. In these systems, higher field strength modifier cations favor the formation of highly charged NBO, over the lower charged bridging oxygens that form linkages such as [4]B–O–[4]Si, thus shifting reaction (3) to the left. The resulting greater concentration of negative charge thus helps stabilize the local coordination environment of the smaller and/or higher charged modifier. Similar boron coordination number changes were found in a variety of borosilicate, aluminoborate and aluminoborosilicate glasses [3,11,42,54,65]. ^{17}O NMR studies have shown that NBO in such systems is most commonly bonded to Si, but that some NBO on borons are present in Ca-rich glasses [42,50]. We also note that higher field strength modifier (or 'charge compensating') cations will also help to stabilize the types of bridging oxygens that have the greatest concentration of negative charge, for example [4]Al–O–[4]Al and [4]B–O–[4]B, whose abundances are generally minimized in systems dominated by large, monovalent cations, as seen directly by ^{17}O NMR [42,66,67]. This effect might tend to stabilize [4]B, a trend opposite of what is seen in most borosilicate systems and in the results presented here. Apparently the mechanism for formation of NBO + [3]B (reaction (3)) is predominant when high cation field strength modifiers are present, especially in glass compositions that are relatively rich in silica, where dilution of B and Al by Si in the network lowers the probability of such highly charged bridging oxygens. However, it has been suggested that the stabilization of [4]B–O–[4]B linkages by small alkali cations (e.g., Li$^+$) in high-alkali binary borate glasses may explain their higher N_4 values relative to those with large alkali cations (e.g., Cs$^+$) [36,51,68]. Steric hindrance for the latter makes charge compensation of such linkages especially difficult [69], perhaps promoting instead the formation of NBO.

A recent, detailed comparison of the effects of K, Na, Ba, Sr, Ca and Mg on network speciation in aluminoborosilicate glasses reported data on a compositional series with fixed modifier oxide and silica contents but varying Al/B [3]. As in our study, a systematic decrease in N_4 was observed with increasing modifier cation charge or decreasing cation radius, and non-linear compositional effects were seen in a CaO–K$_2$O series. The quantization of the ^{11}B NMR results may, however, have been less precise because data were collected by MAS NMR at a much lower field of 7 T; similarly, ^{27}Al MAS NMR at this field could not resolve the [5]Al species. NBO contents were cast in terms of silicate species Q^3 and Q^4 (1 and 0 NBO, respectively), which were in turn derived by fitting of unresolved ^{29}Si MAS NMR spectra. The latter analysis is made somewhat doubtful by the apparently unjustified assumption that the relative proportions of [4]Al, [4]B, and [3]B neighbors to Si (which also change with composition) do not significantly affect the ^{29}Si NMR peak shape or position. Nonetheless, this study provided an interesting analysis of network speciation in terms of an apparent equilibrium constant, K_{app}, for a reaction essentially equivalent to (3) above, which the authors calculated as simply ([Q^4] × [[4]B])/([Q^3] × [[3]B]). Although their data suggest the possibility of effects of Al/B on the value of K_{app}, only constant values and ranges for each modifier were reported, for example 8 ± 3 for Na$_2$O and 0.3 ± 0.1 for CaO. For comparison, the concentrations of Q^4 and Q^3 used for K_{app} can be calculated from our results by assuming that all NBO are coordinated to silicon. This approximation is based on the Dell and Bray model of alkali borosilicate glasses [28] and previous [17]O 3QMAS studies of aluminoborosilicates similar in composition to those described here [42]. Despite differences in the approaches taken to estimating NBO contents between the previous study [3] and ours, a similar trend can be noted: K_{app} for our samples B7N20 (all Na$_2$O) and B7N00 (all CaO) are 5.17 and 0.33, respectively. At higher B/Si (and B/Al), K_{app} values are significantly higher, e.g., for 17.1 for B21N20 (all Na$_2$O) and 0.51 for B21N00 (all CaO). Because of the importance of mixing and order/disorder relationships among the five major network cation species in aluminoborosilicates ([4]Si, [4]Al, [5]Al, [3]B, and [4]B) [42], it is not surprising that composition should systematically effect 'equilibrium constants' of this type, as the extent of mixing will be reflected in the free energy of mixing and hence in activity coefficients for network species.

Related to the effects of modifier cation field strength on boron coordination is a competition for short bonds to oxygen that is well-known to produce more [5]Al in Ca-rich vs. Na-rich aluminosilicates [70,71] and in aluminoborate glasses [53,54]. This effect is also obvious in data presented here and previously [42] that compare alkali and alkaline earth aluminoborosilicates. The apparent non-linearity of the effect of Ca/Na ratio on Al coordination, noted here, resembles trends seen for high-pressure (K, Ca) aluminosilicate glasses [52] and for ambient pressure (Mg, Ca) aluminosilicates [72,73]. It is possibly related to heterogeneous distributions of modifier cations and coordinating oxygens. Such non-linearities in compositional effects on network coordination will be important for accurate empirical or theoretical models of properties.

4.2. Effect of boron content

In Na-rich glasses, lower B/Si ratios produce higher N_4 (Fig. 4). This is expected from extensive NMR studies of the sodium borosilicate system [28], and can be explained at least in part by the decreased probability of [4]B–O–[4]B and of [4]Al–O–[4]B connections, simply by dilution by Si. Because the relatively high negative charges on these types of 'under-bonded' oxygens (formally −1/2) are relatively hard to balance by large, monovalent modifier cations, such bridging oxygens are energetically less favorable than species such as [4]B–O–[4]Si and [4]Al–O–[4]Si (formally −1/4) and [3]B–O–[4]Si and [4]Si–O–[4]Si (formally neutral). In aluminosilicates, this leads to 'Al avoidance'. In Na-rich borosilicates, the network formers are thus relatively ordered because they tend to 'avoid' [4]B–O–[4]B and [4]B–O–[4]Al linkages [14,74], which has been directly observed by recent NMR studies of sodium borosilicate and sodium aluminoborate glasses [45,46,53,63,75]. Unlike aluminosilicates, however, in borosilicates there is another degree of freedom, the conversion of BO$_4$ to BO$_3$ plus NBO, which is thus favored at higher B/Si.

In Ca-rich glasses, the opposite effect is seen. ^{17}O NMR and other data indicate much less tendency towards the chemical ordering described above, because the charges on bridging oxygens

joining two tetrahedral, trivalent cations are easier to balance with Ca^{2+} instead of Na^+ [53,67,76,77]. Species such as $^{[4]}B-O-^{[4]}B$ and $^{[4]}B-O-^{[4]}Al$ may thus actually be stabilized, leading to more N_4 at higher boron content for Ca-rich compositions. Of course, as noted above, Ca^{2+} also stabilizes NBO, leading to more of this species in Ca-rich glasses. In a recent ^{17}O NMR study that specifically addressed these effects [42], mixing of B and Al in a potassium aluminoborosilicate glass tended to follow the $^{[4]}B-O-^{[4]}B$ and $^{[4]}B-O-^{[4]}Al$ avoidance model, but mixing in a Ca aluminoborosilicate of the same stoichiometry (equivalent to sample B7N00 here) was closer to a random mixing model. The data in this study support these conclusions.

For all of the compositions studied here, lower boron concentration leads to considerably higher NBO content (Fig. 4). In borosilicates, both the 'borate-like' modification of network on addition of a modifier oxide, $BO_{3/2} + 1/2O^{2-} = [BO_{4/2}]^-$, and the 'silicate-like' modification, $SiO_{4/2} + 1/2O^{2-} = [SiO_{3/2}O]^-$ are operational. Simply by composition alone, the latter becomes more predominant at higher silica contents: less of the added oxide ion is used to convert $^{[3]}B$ to $^{[4]}B$ and to charge compensate the negatively charged BOs; more of the added oxide is used to convert uncharged BO to charged NBO. Again, however, effects of Ca vs. Na shift the balance in the borate reaction considerably.

4.3. Sodium cation environments

In silicate, borate, and germanate glasses and melts in which Na^+ is the only non-network cation, δ_{iso} for ^{23}Na increases systematically with increasing Na_2O content, in part because of increasing fractions of NBO in the average Na coordination shells and the accompanying shortening of mean Na–O distances [58,78]. However, in the Na–Ca aluminoborosilicates studied here, δ_{iso} for both compositional series *decreases* significantly with increasing NBO content, which results here from increases in CaO/Na_2O. This is likely to result from a strong preference for NBO to coordinate Ca^{2+} instead of Na^+. As CaO/Na_2O increases, more of the oxygens around the Na^+ are BO instead of NBO, even as the total NBO content is increasing. Average Na–O distances are therefore observed to increase. This finding is thus analogous to 'mixed-alkali' effects of modifier cation size [58]. Such non-random distributions of NBO and BO around modifier/charge balancing cations, caused by differences in their field strength, has been observed more directly by ^{17}O NMR in a number of systems, for example recent work on Ca/Mg aluminosilicates [72].

4.4. Other compositional effects

Systematizing the effects of all compositional variables on network speciation in five-component aluminoborosilicate glasses and liquids remains a challenging problem because of the complex effects of mixing of many network species and the apparent non-linearities noted above. We will thus note only a few comparisons. The effects of addition of alumina to the relatively well-known sodium borosilicate system have been explored in several studies [3,9,37,38,40,41,79]. For example, in a recent detailed report on network cation mixing, based on high-resolution ^{11}B, ^{27}Al, and ^{17}O NMR, it was suggested that the similar mixing behavior of $^{[4]}Al$ and $^{[4]}B$ could allow them to be combined together into a single compositional term [42], to be substituted for the B_2O_3 content in the often-applied, empirical 'Dell and Bray' model of the sodium borosilicate system [28]. Although this model cannot hold at high Al/B ratios, it does approximate results for a variety of alkali aluminoborosilicate glasses [37,39,40,42]. Applying this approach to our Na–aluminoborosilicate data (B7N20 and B21N20), the model predicts N'_4 (the sum of $^{[4]}Al + ^{[4]}B$ fractions) as 0.77 and 0.61, vs. measured values of 0.82 and 0.65. This indicates that this empirical

approximation continues to be useful. For alkaline earth rich glasses, however, the major shifts in NBO-producing equilibria produce large divergences from any such model based on alkali oxide compositions. Clearly, a systematic, consistent thermodynamic treatment of these complexities will be needed to yield more accurate structure-based models of bulk properties.

5. Conclusions

In two series of aluminoborosilicates in which CaO/Na_2O is systematically varied, the higher field strength modifier cation (Ca^{2+}) has dramatically different effects on the glass structure when compared to those of the lower field strength cation (Na^+). As CaO/Na_2O increases, the fraction of $^{[4]}B$ decreases greatly, requiring a systematic increase in the fraction of NBO, which are apparently stabilized by the higher modifier cation charge. The same compositional effect also increases the content of $^{[5]}Al$. Variation with composition is non-linear, which may complicate the formulation of predictive models of structure–property relations. Na–O distances on average are longer in high Ca vs. high Na glasses, even though NBO contents are higher, indicating a preference for NBO to be associated with Ca^{2+} and NBO with Na^+.

Acknowledgements

References

[1] Y. Kato, H. Yamazaki, T. Watanabe, K. Saito, A.J. Ikushima, J. Am. Ceram. Soc. 88 (2005) 473.
[2] H. Li, P. Hrma, J.D. Vienna, M.X. Qian, Y.L. Su, D.E. Smith, J. Non-Cryst. Solids 331 (2003) 202.
[3] H. Yamashita, K. Inoue, T. Nakajin, H. Inoue, T. Maekawa, J. Non-Cryst. Solids 331 (2003) 128.
[4] D.S. Wang, C.G. Pantano, J. Non-Cryst. Solids 142 (1992) 225.
[5] V.V. Gerasimov, O.V. Spirina, Glass Ceram. 61 (2004) 168.
[6] T. Maekawa, J. Ceram. Soc. Jpn. 112 (2004) 467.
[7] B. Boizot, N. Ollier, F. Olivier, G. Petite, D. Ghaleb, E. Malchukova, Nucl. Instrum. Methods Phys. Res. Sect. B 240 (2005) 146.
[8] N. Ollier, T. Charpentier, B. Boizot, G. Petite, J. Phys. Condens. Matter 16 (2004) 7625.
[9] H. Yamashita, H. Yoshino, K. Nagata, H. Inoue, T. Nakajin, T. Maekawa, J. Non-Cryst. Solids 270 (2000) 48.
[10] T.M. Besmann, K.E. Spear, J. Am. Ceram. Soc. 85 (2002) 2887.
[11] J.M. Roderick, D. Holland, A.P. Howes, C.R. Scales, J. Non-Cryst. Solids 293 (2001) 746.
[12] R.S. Bubnova, A.A. Levin, N.K. Stepanov, A. Belger, D.C. Meyer, I.G. Polyakova, S.K. Filatov, P. Paufler, Zeit. Krist. 217 (2002) 55.
[13] A.R. Betzen, B.L. Kudlacek, S. Kapoor, J.R. Berryman, N.P. Lower, H.A. Feller, M. Affatigato, S.A. Feller, Phys. Chem. Glasses 44 (2003) 207.
[14] T. Abe, J. Am. Ceram. Soc. 35 (1952) 284.
[15] K. Budhwani, S. Feller, Phys. Chem. Glasses 36 (1995) 183.
[16] I.A. Levitskii, S.A. Gailevich, I.S. Shimchik, Glass Ceram. 61 (2004) 73.
[17] L.C. Protasova, V.C. Kosenko, Glass Ceram. 60 (2003) 164.
[18] N.M. Bobkova, Glass Phys. Chem. 29 (2003) 501.
[19] A.I. Priven, Glass Phys. Chem. 26 (2000) 541.
[20] A.I. Priven, Glass Phys. Chem. 27 (2001) 360.
[21] O.V. Mazurin, J. Non-Cryst. Solids 351 (2005) 1103.
[22] A.I. Priven, Glass Phys. Chem. 26 (2000) 441.
[23] A.V. Loshagin, E.P. Sosnin, Glass Phys. Chem. 20 (1994) 187.
[24] R.J. Araujo, J. Non-Cryst. Solids 58 (1983) 201.
[25] R.J. Araujo, J. Non-Cryst. Solids 81 (1986) 251.
[26] P.J. Bray, R.V. Mulkern, E.J. Holupka, J. Non-Cryst. Solids 75 (1985) 37.
[27] J.H. Zhong, X.W. Wu, M.L. Liu, P.J. Bray, J. Non-Cryst. Solids 107 (1988) 81.
[28] W.J. Dell, P.J. Bray, S.Z. Xiao, J. Non-Cryst. Solids 58 (1983) 1.
[29] Y.H. Yun, P.J. Bray, J. Non-Cryst. Solids 27 (1978) 363.
[30] P.J. Bray, E.J. Holupka, J. Non-Cryst. Solids 71 (1985) 411.
[31] P.K. Gupta, M.L. Lui, P.J. Bray, J. Am. Ceram. Soc. 68 (1985) C82.
[32] S. Kroeker, P.M. Aguiar, A. Cerquiera, J. Okoro, Phys. Chem. Glasses: Eur. J. Glass Sci. Technol. B (2006) 393.
[33] J.F. Stebbins, P.D. Zhao, S. Kroeker, Solid State NMR 16 (2000) 9.

[34] C. Jäger, K. Herzog, B. Thomas, M. Feike, G. Kunath-Fandrei, Solid State NMR 5 (1995) 51.
[35] S. Prabakar, K.T. Mueller, C.G. Pantano, Phys. Chem. Glasses 44 (2003) 125.
[36] G.L. Turner, K.A. Smith, R.J. Kirkpatrick, E. Oldfield, J. Magn. Reson. 67 (1986) 544.
[37] G. El-Damrawi, W. Müller-Warmuth, H. Doweidar, I.A. Gohar, Phys. Chem. Glasses 34 (1993) 52.
[38] W.-F. Du, K. Kuraoka, T. Akai, T. Yazawa, J. Mater. Sci. 35 (2000) 4865.
[39] A.V. Loshagin, E.P. Sosnin, Glass Phys. Chem. 20 (1994) 14.
[40] M. Shim, M. Kang, M. Kim, S. Koo, S. Oh, S. Chung, H. Kim, D. Cha, J. Kor. Phys. Soc. 24 (1991) 426.
[41] F. Angeli, T. Charpentier, S. Gin, J.C. Petit, Chem. Phys. Lett. 341 (2001) 23.
[42] L.-S. Du, J.F. Stebbins, J. Non-Cryst. Solids 351 (2005) 3508.
[43] J.F. Stebbins, J.V. Oglesby, Z. Xu, Am. Mineral. 82 (1997) 1116.
[44] R.E. Youngman, S.T. Haubrich, J.W. Zwanziger, M.T. Janicke, B.F. Chmelka, Science 269 (1995) 1416.
[45] S.H. Wang, J.F. Stebbins, J. Am. Ceram. Soc. 82 (1999) 1519.
[46] L.-S. Du, J.F. Stebbins, J. Phys. Chem. B 107 (2003) 10063.
[47] L.-S. Du, J.F. Stebbins, J. Non-Cryst. Solids 315 (2003) 239.
[48] J.F. Stebbins, S.E. Ellsworth, J. Am. Ceram. Soc. 79 (1996) 2247.
[49] S. Sen, Z. Xu, J.F. Stebbins, J. Non-Cryst. Solids 226 (1998) 29.
[50] T.J. Kiczenski, L.-S. Du, J.F. Stebbins, J. Non-Cryst. Solids 351 (2005) 3571.
[51] J.H. Zhong, P.J. Bray, J. Non-Cryst. Solids 111 (1989) 67.
[52] J.R. Allwardt, J.F. Stebbins, H. Terasaki, L.-S. Du, D.J. Frost, A.C. Withers, M.M. Hirschmann, A. Suzuki, E. Ohtani, Am. Mineral. 92 (2007) 1093.
[53] J.C.C. Chan, M. Bertmer, H. Eckert, J. Am. Ceram. Soc. 121 (1999) 5238.
[54] B.C. Bunker, R.J. Kirkpatrick, R.K. Brow, G.L. Turner, C. Nelson, J. Am. Ceram. Soc. 74 (1991) 1430.
[55] S.K. Lee, J.F. Stebbins, Geochim. Cosmochim. Acta 67 (2003) 1699.
[56] S.C. Kohn, M.E. Smith, P.J. Dirken, E.R.H. van Eck, A.P.M. Kentgens, R. Dupree, Geochim. Cosmochim. Acta 62 (1998) 79.
[57] B.C. Schmidt, T. Riemer, S.C. Kohn, H. Behrens, R. Dupree, Geochim. Cosmochim. Acta 64 (2000) 513.
[58] J.F. Stebbins, Solid State Ionics 112 (1998) 137.
[59] X.Y. Xue, J.F. Stebbins, Phys. Chem. Mineral. 20 (1993) 297.
[60] A.M. George, J.F. Stebbins, Am. Mineral. 80 (1995) 878.
[61] A.M. George, S. Sen, J.F. Stebbins, Solid State NMR 10 (1997) 9.
[62] J.F. Stebbins, E.V. Dubinsky, K. Kanehashi, K.E. Kelsey, Geochim. Cosmochim. Acta 72 (2008) 910.
[63] L.-S. Du, J.F. Stebbins, Solid State NMR 27 (2005) 37.
[64] N.M. Bobkova, Z.V. Apanovich, S.A. Gailevich, J. Appl. Spectrosc. 47 (1987) 743.
[65] M.E. Fleet, S. Muthupari, J. Non-Cryst. Solids 255 (1999) 233.
[66] S.K. Lee, J.F. Stebbins, J. Non-Cryst. Solids 270 (2000) 260.
[67] S.K. Lee, J.F. Stebbins, Am. Mineral. 84 (1999) 937.
[68] V.K. Michaelis, P.M. Aguiar, S. Kroeker, J. Non-Cryst. Solids 353 (2007) 2582.
[69] B.O. Mysen, Silicate Glasses and Melts: Properties and Structure, Elsevier, Amsterdam, 2005.
[70] S.K. Lee, G.D. Cody, B.O. Mysen, Am. Mineral. 90 (2005) 1393.
[71] J.R. Allwardt, J.F. Stebbins, B.C. Schmidt, D.J. Frost, A.C. Withers, M.M. Hirschmann, Am. Mineral. 90 (2005) 1218.
[72] K.E. Kelsey, J.F. Stebbins, L.-S. Du, J.L. Mosenfelder, P.D. Asimow, C.A. Geiger, Am. Mineral. 93 (2008) 134.
[73] D.R. Neuville, L. Cormier, V. Montouillout, P. Florian, F. Millot, J.-C. Rifflet, D. Massiot, Am. Mineral. 93 (2008) 1721.
[74] R.J. Araujo, J. Non-Cryst. Solids 42 (1980) 209.
[75] M. Bertmer, L. Züchner, J.C.C. Chan, H. Eckert, J. Phys. Chem. B 104 (2000) 6541.
[76] J.F. Stebbins, Z. Xu, Nature 390 (1997) 60.
[77] S.K. Lee, J.F. Stebbins, J. Phys. Chem. B 104 (2000) 4091.
[78] L.M. Peng, J.F. Stebbins, J. Non-Cryst. Solids 353 (2007) 4732.
[79] K.L. Geisinger, R. Oestrike, A. Navrotsky, G.L. Turner, R.J. Kirkpatrick, Geochim. Cosmochim. Acta 52 (1988) 2405.